https://doi.org/10.5194/acp-2022-419
Preprint. Discussion started: 24 June 2022

Atmospheric Chemistry and Physics Discussions

Quantifying the Importance of Vehicle Ammonia Emissions in an Urban Area of the Northeastern US Utilizing Nitrogen Isotopes

Wendell W. Walters[*1,2], Madeline Karod[1,3], Emma Willcocks[4], Bok H. Baek[5], Danielle E. Blum[2,6], and Meredith G. Hastings[1,2]

[1]Department of Earth, Environmental, and Planetary Sciences, Brown University; Providence, RI 02912, USA.
[2]Institute at Brown for Environment and Society, Brown University; Providence, RI 02912, USA
[3]Chemistry and Physics Department, Simmons University; Boston MA 02215, USA
[4]Program in Biology, Division of Biology and Medicine, Brown University; Providence, RI 02912, USA
[5]Center for Spatial Information, Sciences, and Systems, George Mason University; Fairfax, VA 22030, USA
[6]Department of Chemistry, Brown University; Providence, RI 02916, USA

Correspondence to: Wendell W. Walters (wendell_walters@brown.edu)

Abstract. Atmospheric ammonia (NH_3) is a critical component of our atmosphere that contributes to air quality degradation and reactive nitrogen deposition; however, our knowledge of NH_3 in urban environments remains limited. Year-long ambient NH_3 and related species were measured for concentrations and the nitrogen isotopic compositions ($\delta^{15}N$) of NH_3 and particulate ammonium (pNH_4^+) to understand the temporal sources and chemistry of NH_3 in a northeastern US urban environment. We found that urban NH_3 and pNH_4^+ concentrations were elevated compared to regional rural background monitoring stations, with seasonally significant variations. Local and transported sources of NH_x (NH_3 + pNH_4^+) were identified using polar bivariate and statistical back trajectory analysis, which suggested the importance of vehicles, volatilization, industry, fuel combustion, and biomass burning emissions. Utilizing a uniquely positive $\delta^{15}N(NH_3)$ emission source signature from vehicles, a Bayesian stable isotope mixing model indicates that vehicles contribute 30.7±11.6% (mean±1σ) to the annual background level of urban NH_x, with a strong seasonal pattern with higher relative contribution during winter (45.8±13.0%) compared to summer (20.8±9.7%). The decrease in the relative importance of vehicle emissions during the summer was suggested to be driven by temperature-dependent NH_3 emissions from volatilization sources based on wind direction, back trajectory, and NH_3 emission inventory analysis. This work highlights that reducing vehicle NH_3 emissions should be considered to improve wintertime air quality in this region.

https://doi.org/10.5194/acp-2022-419
Preprint. Discussion started: 24 June 2022

Atmospheric Chemistry and Physics Discussions

1. Introduction

Ammonia (NH_3) is a critical component of the atmosphere and the global nitrogen cycle (Behera et al., 2013; Galloway et al., 2004). As the primary alkaline atmospheric molecule, NH_3 plays an important role in neutralizing atmospheric acids, leading to fine particulate matter ($PM_{2.5}$), including particulate ammonium (pNH_4^+), which have important implications for air quality, human health, visibility, and climate change (Behera and Sharma, 2010; Updyke et al., 2012; Wang et al., 2015). Agricultural activities, including fertilizer application and livestock waste, dominate the emission of NH_3, accounting for over 60% of the global inventory (Bouwman et al., 1997); however, there are significant NH_3 spatiotemporal variabilities due to its short atmospheric lifetime, typically a few hours to a day, and numerous emission sources (Van Damme et al., 2018). Urban regions have been shown to have elevated levels of NH_3 and reduced nitrogen deposition (Plautz, 2018; Joyce et al., 2020; Hu et al., 2014; Decina et al., 2020, 2017), indicating the potential for important non-agricultural emission sources that may disproportionately impact human and environmental health. In recent years, quantifying surface-level NH_3 and its deposition products in the US has been a focus of several national monitoring networks, including the Ammonia Monitoring Network (AMoN), the Interagency Monitoring of Protected Visual Environments (IMPROVE), the National Atmospheric Deposition Program (NADP), and the Clean Air Status and Trends Network (CASTNET). However, these measurements are typically conducted in rural locations. Long-term records of NH_3 and its deposition products in urban regions are exceedingly scarce, which often leads to models evaluated to observations primarily conducted in rural locations.

The NH_3 sources contributing to the urban budget remain contested. Several studies have identified vehicle emissions as a major urban NH_3 emission source (Sun et al., 2017, 2014; Suarez-Bertoa et al., 2014, 2017). In contrast, other studies have suggested that vehicle emissions are relatively unimportant for urban regions and instead have found evidence for significant local and transported emissions due to temperature-dependent volatilization sources (Hu et al., 2014; Yao et al., 2013; Nowak et al., 2006). Recent satellite observations, taking advantage of the COVID-19 lockdown period, have for the first time confirmed vehicle emissions as a significant localized source of NH_3 in an urban region (Cao et al., 2021). However, quantifying the contribution of local urban NH_3 emissions to the urban background is complex as it is coupled to meteorological

https://doi.org/10.5194/acp-2022-419
Preprint. Discussion started: 24 June 2022


Atmospheric Chemistry and Physics Discussions

parameters that influence NH_3 and particulate ammonium (pNH_4^+) partitioning, mixing/dispersion of local emissions, and contributions via long-range transport from agricultural regions (Meng et al., 2011; Walker et al., 2004).

The nitrogen stable isotopic composition ($\delta^{15}N(‰) = [(^{15}R_{sample})/(^{15}R_{reference})-1]\times1000$, where ^{15}R is the ratio of $^{15}N/^{14}N$, and air is the N isotopic reference) may be a useful chemical fingerprinting tool to track source contributions and validate model apportionments of urban NH_3 (Felix et al., 2017, 2013). Indeed, numerous studies have utilized $\delta^{15}N$ of NH_3 and pNH_4^+ for source apportionment (Felix et al., 2017; Pan et al., 2016; Berner and Felix, 2020; Liu et al., 2018; Pan et al., 2018; Wu et al., 2019; Bhattarai et al., 2020; Xiao et al., 2020; Zhang et al., 2021), taking advantage of the suggested lower $\delta^{15}N$ signatures of agricultural NH_3 emissions relative to fossil fuel combustion (Felix et al., 2013; Chang et al., 2016). However, it has been shown that collection techniques can play an important role on the measured $\delta^{15}N$ values (Skinner et al., 2006). Passive collection of NH_3 has been shown to induce a $\delta^{15}N$ bias relative to active collection techniques due to a potential diffusion isotope effect, such that many of the $\delta^{15}N(NH_3)$ studies may be unreliable (Walters et al., 2020; Pan et al., 2020; Kawashima et al., 2021; Crittenden et al., 2015). Additionally, collections of pNH_4^+ on aerosol filters may be impacted by the loss of semi-volatile NH_4NO_3 leading to an undesirable $\delta^{15}N$ fractionation (Walters et al., 2019). Thus, there could be inaccuracies in the previously reported source apportionment results related to the collection technique used to concentrate ambient NH_3 and pNH_4^+ for offline $\delta^{15}N$ characterization.

An additional complication for utilizing $\delta^{15}N$ for source apportionment is the role of isotope fractionation associated with NH_3 and pNH_4^+ phase partitioning (Urey, 1947). This phase partitioning is driven by a thermodynamic equilibrium that depends on the relative humidity, temperature, and particle chemical composition and is typically achieved on the order of tens of minutes (Meng and Seinfeld, 1996). This suggests that isotope equilibrium between NH_3 and pNH_4^+ should be achieved under most ambient atmosphere conditions. Absorption of NH_3 in a deliquesced particle can be represented by the following (R1):

$$NH_{3(g)} + H_2O_{(l)} \leftrightharpoons NH_3 * H_2O \leftrightharpoons NH_{4(aq)}^+ + OH^- \qquad \text{R1}$$

The associated $NH_{3(g)}$-$pNH_4^+{}_{(aq\ or\ s)}$ nitrogen equilibrium isotope exchange has been suggested to be represented through the following reactions (Walters et al., 2018; Urey, 1947) (R2-R4):

https://doi.org/10.5194/acp-2022-419
Preprint. Discussion started: 24 June 2022

Atmospheric Chemistry and Physics Discussions

$$^{15}NH_{3(g)} + {}^{14}NH^{+}_{4(s)} \rightleftharpoons {}^{14}NH_{3(g)} + {}^{15}NH^{+}_{4(s)} \quad \text{R2}$$

$$^{15}NH_{3(g)} + {}^{14}NH^{+}_{4(aq)} \rightleftharpoons {}^{14}NH_{3(g)} + {}^{15}NH^{+}_{4(aq)} \quad \text{R3}$$

$$^{15}NH_{3(g)} + {}^{14}NH_{3(aq)} \rightleftharpoons {}^{14}NH_{3(g)} + {}^{15}NH_{3(aq)} \quad \text{R4}$$

Recent theoretical calculations predict nitrogen equilibrium constants (K) or isotopic fractionation factors (α) of 1.031(±0.004), 1.034(±0.004), and 1.004(±0.003) at 25 °C for R2, R3, and R4, respectively (Walters et al., 2018). These calculations indicate that isotope equilibrium will lead to the preferential partitioning of ^{15}N in the condensed phase of NH_x with an isotopic enrichment factor (ε(‰) = 1000[α-1]) ranging from 4.0 to 34‰ depending on the equilibrium reaction (Walters et al., 2018). Previous work has also suggested that unidirectional NH_3 neutralization reactions involving sulfuric acid (H_2SO_4) may induce a kinetic isotope effect of approximately -28‰ (Pan et al., 2016). These potential competing equilibrium and kinetic isotope effects indicate that the phase $\delta^{15}N$ fractionation between NH_3 and pNH_4^+ is complex. However, most previous $\delta^{15}N(NH_3)$ source apportionment studies have collected a single phase of NH_x and have either not considered $\delta^{15}N$ fractionation or estimated the effect based on only NH_3/NH_4^+ equilibrium exchange reactions (R2 & R3). This may not be a robust approach due to the wide range of $\delta^{15}N$ fractionation predicted from equilibrium and/or kinetic isotope effects (i.e., -28 to 34‰), leading to inaccurate source apportionment results. Indeed, laboratory dynamic flow chamber experiments and field measurements from simultaneously collected NH_3 and pNH_4^+ have reported lower ε than calculated for R2 and R3 (Walters et al., 2019; Kawashima and Ono, 2019). Thus, predicting the isotope fractionation factor associated with NH_3 and pNH_4^+ phase partitioning under varying ambient conditions remains unclear (Bhattarai et al., 2021), implying that speciated and simultaneous collections of NH_x is needed to account for the complex NH_3/pNH_4^+ fractionation to reduce the influence of phase-dependent $\delta^{15}N$ variabilities.

Improving the reliability of $\delta^{15}N$ source apportionment results of NH_3 requires using robust methods suitable for $\delta^{15}N$ characterization that can also account for phase-dependent $\delta^{15}N$ variabilities. In this study, we have characterized the seasonal ambient NH_x (NH_3 + pNH_4^+) source contributions using concentration and isotope measurements at an urban site in Providence, RI, US, using laboratory-verified and field-tested collection techniques shown to quantitatively collect NH_x for accurate and precise $\delta^{15}N$ characterizations (Walters and Hastings, 2018; Walters et al., 2019). The study site is a mid-sized

https://doi.org/10.5194/acp-2022-419
Preprint. Discussion started: 24 June 2022


Atmospheric Chemistry and Physics Discussions

coastal city located within the northeastern US megapolis. This is an important region to monitor because the northeastern US wintertime air quality has not improved as much as expected, despite aggressive reductions of precursor emissions in recent decades (Shah et al., 2018). We have recently characterized the $\delta^{15}N(NH_3)$ from urban vehicle plumes, which has indicated this source to have a unique positive $\delta^{15}N$ signature of 6.6±2.1‰ compared to other NH_3 sources that tend to have negative $\delta^{15}N$ values (Walters et al., 2020). Here we aim to quantify the importance of vehicle NH_3 emissions at our urban site. Our study contributes to the first $\delta^{15}N$ measurements of speciated NH_x in New England and contributes to our understanding of seasonal urban NH_x source apportionment in an environment that particulate nitrate (pNO_3^-) formation is commonly NH_3-limited (Park et al., 2004).

2. Materials, Methods, and Datasets

2.1 Collection of NH_x and Associated Gases and Particles

Simultaneous collections of reactive gases and $PM_{2.5}$ were conducted using a series of coated glass honeycomb denuders and a downstream filter pack housed in a ChemComb Speciation Cartridge. This sampling system has been extensively evaluated for its ability to speciate between inorganic gases and particulate matter for offline concentration determination (Koutrakis et al., 1993, 1988). Additionally, this system is a suitable technique for the characterization of $\delta^{15}N(NH_3)$ and $\delta^{15}N(pNH_4^+)$ with a precision of ±0.8‰ and ±0.9‰ (1σ), respectively (Walters and Hastings, 2018; Walters et al., 2019). Briefly, the sampler consisted of a PTFE-coated inlet to minimize reactive gas loss, a $PM_{2.5}$ impactor plate, a basic-coated honeycomb denuder (2% carbonate (w/v) + 1% glycerol (w/v) in 80:20 water-methanol (v/v) solution) to collect acidic gases including nitric acid (HNO_3) and sulfur dioxide (SO_2), an acid-coated denuder (2% citric acid (w/v) + 1% glycerol (w/v) in 20:80 water-methanol (v/v) solution) to collect NH_3, and a filter pack consisting of a Nylon and 5% (w/v) citric acid-coated cellulose filter for the collection of pNH_4^+. All denuder and filter preparation, handling, and extraction techniques have been previously described (Walters and Hastings, 2018; Walters et al., 2019). The samplers were held vertically to limit the potential for gravitational settling of particles on the denuder surfaces and were housed in a custom-built weather-protected container. Ambient air was sampled at a flow rate of 10 liters per minute. Collections were conducted for 24 h (15:00 to 15:00 the following day) approximately twice per week in Providence, RI, US (41.83 ºN, 71.40 ºW) on the rooftop of a building from February 6, 2018, to February 1, 2019 (Figure 1). The study location is a mid-sized coastal city within New England, with an approximate population of 180,000 and population density of 3,800 per km^2. The monitoring location is in an urban-mixed use region that includes commercial buildings, residential buildings, highways, and industry with some clear NH_3 point sources such as vehicles, residential heating, sewage, and industrial emission.

https://doi.org/10.5194/acp-2022-419
Preprint. Discussion started: 24 June 2022


Atmospheric Chemistry and Physics Discussions

2.2 Concentration and $\delta^{15}N(NH_x)$ Isotopic Analysis

The concentrations of the denuder and filter extraction solutions were analyzed using colorimetry and ion chromatography analytical techniques. The colorimetric analysis included measurements of [NH_4^+] using the indophenol blue method (i.e., US EPA Method 350.1) and [NO_2^-] via diazotization with sulfanilamide dihydrochloride (i.e., US EPA Method 353.2) that was automated by a discrete UV-Vis spectrophotometer (Westco SmartChem). Anion concentrations that included [Cl^-], [NO_3^-], and [SO_4^{2-}] were analyzed using ion chromatography (Dionex DX500). The limit of detection (LOD) of was approximately 0.5 μmol·L^{-1} for [NH_4^+] and [NO_2^-] and 2 μmol·L^{-1} for [Cl^-], [NO_3^-], and [SO_4^{2-}]. The relative standard deviations for all quantified ions were less than 5%. Laboratory blanks of denuder and filter samples were periodically taken, representing approximately 10% of the collected samples. The blanks were below our LOD, except for [Cl^-] that had a large and variable blank for both the carbonate denuder and Nylon filter, such that this data was not reported in this work.

The determination of $\delta^{15}N$ of the NH_4^+ in the denuder and filter extracts was conducted using a chemical technique that converts NH_4^+ to NO_2^- using an alkaline hypobromite solution and reducing the generated NO_2^- to N_2O using sodium azide in an acetic acid buffer solution (Zhang et al., 2007). The generated N_2O was purified and concentrated using an automated extraction system coupled to a continuous flow Isotope Ratio Mass Spectrometer for $\delta^{15}N$ determination as previously described (Walters and Hastings, 2018). In each sample batch, unknowns were calibrated to two internationally recognized NH_4^+ isotopic reference materials, IAEA-N2 and USGS25, with $\delta^{15}N$ values of 20.3‰ and -30.3‰ (Bohlke et al., 1993; Böhlke and Coplen, 1993), respectively. An in-house NH_4^+ quality control ($\delta^{15}N$ = -1.5‰) and an NO_2^- reference material with a known isotope composition (RSIL-N10219; $\delta^{15}N$= 2.8‰) (Böhlke et al., 2007) were also run intermittently as quality control to monitor the conversion of NO_2^- to N_2O and system stability across runs. Corrections to determine $\delta^{15}N(NH_4^+)$ are performed by accounting for isobaric influences, blank effects, and calibrating the unknowns to the internationally recognized $\delta^{15}N(NH_4^+)$ standards. The correction scheme resulted in an average slope between the measured $\delta^{15}N(N_2O)$ and the standard $\delta^{15}N(NH_4^+)$ values of 0.501 ± 0.024 near the theoretical line of 0.500 for the azide/acetic acid reduction method (Zhang et al., 2007; McIlvin and Altabet, 2005). The pooled standard deviations of the isotopic reference materials were ±0.6‰ (n=62), ±0.7‰ (n=62), ±0.5‰ (n=14), and ±1.3‰ (n=18), for IAEA-N2, USGS25, in-house NH_4^+, and RSIL-N10219, respectively. Due to the numerous steps and potential interferences associated with the employed chemical conversion technique, we established the following quality assurance criteria for our sample unknowns: (1) [NH_4^+] greater than 5 μmol·L^{-1} to combat the significant alkaline hypobromite reagent blank, (2) [NO_2^-]/[NH_4^+] ratio less than 5% since NO_2^- is an interferent, and (3) quantitative yield of NH_4^+ to NO_2^- conversion (i.e., incomplete conversion would lead to undesirable $\delta^{15}N$ fractionation). These criteria were met for 89 out of 97 NH_3 samples and 60 out of 97 pNH_4^+ samples. Replicate measurements of sample unknowns across batch analyses was conducted for approximately 10% of samples and had an average deviation of ±1.4‰.

https://doi.org/10.5194/acp-2022-419
Preprint. Discussion started: 24 June 2022


Atmospheric Chemistry and Physics Discussions

170

2.3 Ancillary Datasets

Annual emission data of NH_3 at the county level was accessed from the US EPA National Emission Inventory 2014 (NEI-14), and chemically speciated gridded hourly NH_3 emission data was generated using the Sparse Matrix Operator Kerner Emissions (SMOKE) model (Baek and Seppanen, 2021). The SMOKE processor was initialized using the NEI-2014 emissions modeling
175 platform (EMP) version 7.1, as this was the most recently available NEI at the time of the analysis. The model output was binned by month. Ancillary meteorological parameters were accessed from the Rhode Island Department of Health air monitoring and Chemical Speciation Network (CSN) monitoring station at East Providence (Figure 1). Data were accessed from co-located Ammonia Monitoring Network (AMoN) and Clean Air Status and Trends Network (CASTNET) stations located within New England (US EPA Region 1) for [NH_3] and [pNH_4^+], respectively. These sites included Abington, CT
180 (41.84ºN, 72.01°W), Underhill, VT (44.53ºN, 72.87°W), Woodstock, NH (44.53ºN, 72.87°W), and Ashland, ME (46.60ºN, 68.41°W) (Figure 1). Archived back trajectories and boundary layer heights were computed using the NOAA Air Resource Lab HYSPLIT model (Stein et al., 2015). 72-h back trajectories were calculated arriving at Providence, RI (41.73°N, 71.43°W) using the NAM 12 km meteorology initiated at the end of each sampling period. Atmospheric NH_x has a lifetime typically on the order of 2.1 days (Paulot et al., 2016), such that the chosen trajectory time should account for the potential of long-range
185 transport of NH_x to the sampling site. A new back trajectory was calculated every 3 h for a max of 8 trajectories encompassing the 24 h sampling period at 100 m above ground level.

2.4 Statistical Analyses

Geospatial statistical analysis that included bivariate wind direction and wind speed polar plots and back-trajectory clustering
190 was conducted using the 'open-air' program package using R (Carslaw and Ropkins, 2012). Local NH_x source identification was estimated using the conditional bivariate probability function (CBPF) analysis that provides a conditional probability field for high concentrations dependent on wind speed and direction (Uria-Tellaetxe and Carslaw, 2014). It is defined as the following (Eq. 1):

$$CBPF_{\Delta\theta,\Delta u} = \frac{m_{\Delta\theta,\Delta u|C\geq x}}{n_{\Delta\theta,\Delta u}} \qquad \text{(Eq. 1)}$$

195 where $m_{\Delta\theta,\Delta u}$ is the number of samples in the wind sector $\Delta\theta$ with wind speed interval Δu having concentration C greater than a threshold value x, $n_{\Delta\theta,\Delta u}$ is the total number of samples in that wind direction-speed interval. The threshold values were set as the top 25% concentration for these analyses. These bivariate polar plots show how a concentration of species varies with wind speed and direction in polar coordinates and are useful in characterizing emission sources (Carslaw and Ropkins, 2012; Carslaw et al., 2006; Tomlin et al., 2009; Zhou et al., 2019). Additionally, source locations that contribute to long-range NH_x
200 transport were evaluated using the potential source contribution function (PSCF). This analysis combines atmospheric

https://doi.org/10.5194/acp-2022-419
Preprint. Discussion started: 24 June 2022


Atmospheric Chemistry and Physics Discussions

concentrations with air mass trajectories and uses residence time information to identify air parcels that contribute to high concentrations at a receptor site (Fleming et al., 2012; Pekney et al., 2006; Begum et al., 2005). The PSCF calculation indicates the probability that a source is located at latitude *i* and longitude *j* and is calculated as the following (Eq. 2):

$$PSCF = \frac{m_{ij}}{n_{ij}} \quad \text{(Eq. 2)}$$

where n_{ij} is the number of times that the trajectories pass through the cell (i,j) and m_{ij} is the number of times that a source concentration was high when the trajectories passed through the cell (i,j), and the criterion for determining m_{ij} was defined as the 90th percentile (Carslaw and Ropkins, 2012).

3. Results and Discussion

3.1 Urban NH_3 and pNH_4^+ Temporal Concentrations

The urban NH_3 and pNH_4^+ were monitored under a range of meteorological conditions (Figure 2). The annual [NH_3] ranged from 0.234 to 2.94 μg/m^3 with a mean of 0.890±0.517 μg/m^3 (n=97), and [pNH_4^+] ranged from 0.019 to 1.62 μg/m^3 with a mean of 0.412±0.287 μg/m^3. The NH_x partitioning between gas and particle-phase was quantified as fNH_3 (fNH_3 = $[NH_3]_{mol}/([NH_3]_{mol} + [pNH_4^+]_{mol})$ and ranged from 0.307 to 0.972 with an average of 0.688±0.141 (n=97). A strong seasonal pattern was observed for both [NH_3] and fNH_3, with the highest values observed during warmer periods. No significant seasonal pattern was observed for [pNH_4^+] that remained relatively consistent throughout each season and characterized by frequent spike events in cold and warm months, including near July 4th, corresponding to a period of significant firework activity.

The [NH_3] and fNH_3 were positively correlated with temperature ($r = 0.66$; $p<0.01$ & $r = 0.51$; $p<0.01$; Figure S1). This relationship was consistent with previous observations in rural and urban locations that suggested [NH_3] to be influenced by temperature-dependent volatilization (e.g., agriculture, vegetation, sewage, and waste) and evaporation from semi-volatile NH_4NO_3 particles (Wang et al., 2015; Hu et al., 2014; Yao et al., 2013; Nowak et al., 2006; Yao and Zhang, 2016). Additionally, [NH_3] was negatively correlated with wind speed ($r = -0.42$; $p < 0.01$) and mixing height ($r = -0.52$; $p<0.01$) indicating the importance of dilution and vertical height to near-surface [NH_3]. The measured [pNH_4^+] were not significantly correlated with any meteorological parameter (Figure S1). Instead, the annual and seasonal [pNH_4^+] was closely associated with [pNO_3^-] ($r=0.69$; $p<0.01$) and [pSO_4^{2-}] ($r=0.63$; $p<0.01$). This finding is expected due to the role that NH_3 has in neutralizing atmospheric nitric acid and sulfuric acid, leading to pNH_4^+ aerosols in the form of NH_4NO_3, NH_4HSO_4, and NH_4SO_4.

https://doi.org/10.5194/acp-2022-419
Preprint. Discussion started: 24 June 2022


Atmospheric Chemistry and Physics Discussions

3.2 Comparison of Urban NH_3 and pNH_4^+ to Regional Observations

The measured urban [NH_3] and [pNH_4^+] data from Providence, RI, US was compared with the nearby regional observations from AMoN/CASTNET sites within New England (Figure 1 & Figure 3). Overall, the annual average [NH_3] in Providence, RI, was significantly greater ($p<0.05$) than the regional New England AMoN sites; however, [NH_3] grouped by season indicates subtle differences in the seasonal profiles at the varying New England sites (Figure 3A). [NH_3] at Providence, RI was statistically higher ($p<0.05$) during winter and autumn than the New England AMoN sites and higher than all sites except for Abington, CT, during summer. During spring, [NH_3] at Providence, RI, was not statistically different from any of the New England AMoN sites, which typically exhibited a springtime [NH_3] peak that likely reflects the influence and timing of fertilization application (Felix et al., 2017). We note that there can be large heterogeneity in urban [NH_3]; however, the Providence, RI monitoring site was specifically chosen since it was away from any direct emission sources and at a raised elevation. The difference in our measured [NH_3] and reported by AMoN are unlikely to be explained by differences in sampling methodology. We have recently demonstrated that our active denuder sampling technique resulted in NH_3 concentrations within 2-5% of that determined from simultaneous deployed passive NH_3 collection techniques, which are utilized at AMoN sites (Walters et al., 2020). This result was consistent with previous comparisons between active and passive NH_3 sampling techniques (Zhou et al., 2019; Puchalski et al., 2015).

The annual average [pNH_4^+] at the Providence, RI site was also found to be significantly higher than the regional CASTNET sites ($p<0.05$; Fig. 3B). However, when broken down by season, the Providence, RI site has significantly higher [pNH_4^+] than all the regional CASTNET sites only during autumn ($p<0.05$), suggesting that [pNH_4^+] may be more regional representative than [NH_3] due to its extended atmospheric lifetime relative to NH_3 (Paulot et al., 2016). During the winter and summer, the Providence, RI site did not have significantly higher [pNH_4^+] than any of the CASTNET sites. During the spring, [pNH_4^+] was higher in Providence, RI, than the two most remote regional CASTNET sites, including Ashland, ME, and Woodstock, NH ($p<0.05$), but not significantly different from the Abington, CT or Underhill, VT sites. It is important to note that methodology differences in the collection of pNH_4^+ could have significantly influenced the [pNH_4^+] annual differences and seasonal patterns. Our collection method (Nylon filter + acid-coated filter) should lead to the quantitative collection of pNH_4^+ (Walters et al., 2019; Yu et al., 2006). In contrast, pNH_4^+ collections at the CASTNET sites utilize PTFE filters which could be biased low due to the potential for significant loss of semi-volatile NH_4NO_3 (Ashbaugh and Eldred, 2004; Yu et al., 2005). The potential for NH_4NO_3 volatilization should be more significant for warmer temperatures (Ashbaugh and Eldred, 2004; Yu et al., 2005). However, we did not observe a significant difference in summer [pNH_4^+] between the Providence, RI, and regional CASTNET sites. Thus, the influence of sampling methodologies on the spatiotemporal [pNH_4^+] patterns remains difficult to quantify.

https://doi.org/10.5194/acp-2022-419
Preprint. Discussion started: 24 June 2022


Atmospheric Chemistry and Physics Discussions

Localized NH_3 emissions likely play an important role in contributing to the observed elevated urban [NH_x] and the spatiotemporal patterns across New England (Figure 4). The NEI-14 emission profiles at the AMoN sites indicated that agricultural activities drive the seasonal NH_3 emissions, while non-agricultural sources, including stationary fuel combustion (electricity generating units and residential heating) and vehicles, were important during winter but their relative contributions significantly decreased during warmer periods. In contrast, the annual NH_3 emission in Providence, RI were dominated by fuel combustion emissions. The total NH_3 emission density in Providence, RI had less seasonal variability than the regional AMoN/CASTNET locations despite a potential seasonal change in emissions with relatively high contributions from residential heating (i.e., oil, gas, wood combustion) during winter compared with summer. We note that natural gas and oil stationary fuel combustion, which is predicted to be the main NH_3 emission source at our urban study site as well as in other major urban areas in regions with a large heating demand (Zhou et al., 2019), has a highly uncertain NH_3 emission factor established from limited studies conducted before 1982 (Muzio and Arand, 1976; Cass et al., 1982). Additionally, it has been recently pointed out that vehicle NH_3 emission, another major source of urban NH_3, might be underpredicted by at least a factor of 2 in the NEI (Sun et al., 2017; Fenn et al., 2018).

3.3 Urban $\delta^{15}N$ of Urban NH_x

Measurements of $\delta^{15}N$ at the Providence, RI monitoring site were utilized to enhance understanding of source contributions to urban NH_x. The measured $\delta^{15}N(NH_3)$ ranged from -21.4 to -2.0‰ with an average of -11.9±5.0‰ (n=90), and $\delta^{15}N(pNH_4^+)$ ranged from -7.4 to 17.5‰ with a mean of 4.9±6.2‰ (n=60) (Figure 5). The measured $\delta^{15}N$ data was binned by season that included winter (Dec, Jan, Feb), spring (Mar, Apr, May), summer (Jun, Jul, Aug), and autumn (Sep, Oct, Nov). The $\delta^{15}N(NH_3)$ was statistically higher during spring (-7.6±3.5‰, n=21 ($\bar{x}$±1σ)) compared to the other seasons (summer = -13.9±4.1‰, n=21; autumn = -13.1±5.1‰, n=21; winter = -13.4±5.2‰, n=18, $p<0.05$). The $\delta^{15}N(pNH_4^+)$ also indicated significant seasonality with lower values during summer (0.4±4.9‰, n=18) compared to autumn (7.4±4.8‰, n=15) and winter (9.0±5.8‰; n=14) ($p<0.05$). However, springtime $\delta^{15}N(pNH_4^+)$ (4.1±5.2‰, n=13) was not statistically different from any season.

The $\delta^{15}N$ of atmospheric NH_3 and pNH_4^+ reflects a combination of source effects from different NH_3 emission sources and isotopic equilibrium between NH_3 and pNH_4^+ that has been shown to have a large influence on setting the N isotopic distribution between these molecules (Walters et al., 2018; Savard et al., 2017; Kawashima and Ono, 2019). Indeed, the annual $\delta^{15}N(pNH_4^+)$ was statistically higher than $\delta^{15}N(NH_3)$ ($p<0.01$), reflecting the contributions from the nitrogen isotope exchange reactions between NH_3 and NH_4^+ (R2-R4), which tends to elevate the $\delta^{15}N(pNH_4^+)$ relative to $\delta^{15}N(NH_3)$ (Walters et al., 2018; Kawashima and Ono, 2019; Urey, 1947). The isotope difference or isotope enrichment factor ($^{15}\varepsilon_{pNH4+/NH3}$) between $\delta^{15}N(pNH_4^+)$ and $\delta^{15}N(NH_3)$ was calculated as the following (Eq. 3):

$$\Delta\delta^{15}N \approx {}^{15}\varepsilon_{pNH_4^+/NH_3} = \delta^{15}N(pNH_4^+) - \delta^{15}N(NH_3) \qquad \text{(Eq. 3)}$$

https://doi.org/10.5194/acp-2022-419
Preprint. Discussion started: 24 June 2022


Atmospheric Chemistry and Physics Discussions

The $\Delta\delta^{15}N$ ranged from -0.1 to 34.1‰ and averaged 17.6±7.8% (n=56) (Figure S2). The wide range of $\Delta\delta^{15}N$ values was generally within the varying NH_x isotope equilibrium reactions (R2-R4) (Walters et al., 2018). However, kinetic isotope fractionation and fresh NH_3 emissions that might perturb the NH_3/pNH_4^+ isotope equilibrium may also play a role (Pan et al., 2016). The $\Delta\delta^{15}N$ were weakly correlated with temperature (r = -0.55, p <0.01) and $[pNO_3^-]$ (r = 0.33, p<0.05), suggesting that these values were difficult to predict. This result has important implications for previous $\delta^{15}N$ source apportionment studies of NH_3 and pNH_4^+, which commonly utilize an assumed and theoretically calculated phase-dependent fractionation.

To account for the complex phase-dependence on $\delta^{15}N$ variabilities, we calculated $\delta^{15}N(NH_x)$ according to the following (Eq. 4):

$$\delta^{15}N(NH_x) = fNH_3 \times \delta^{15}N(NH_3) + (1 - fNH_3) \times \delta^{15}N(NH_4^+) \quad \text{(Eq. 4)}$$

The annual $\delta^{15}N(NH_x)$ ranged from -17.4 to 6.3‰ and averaged -6.0±4.9‰ (n=56) (Figure 5). There was significant seasonality with lower values during summer (-9.0±4.2‰, n=18) compared to winter (-3.4±5.3‰, n=13) and spring (-3.8±3.3‰, n=10). The autumn $\delta^{15}N(NH_x)$ (-6.2±4.1‰, n=15) was not significantly different from any season. The $\delta^{15}N(NH_x)$ is independent of the phase $\delta^{15}N$ fractionation, such that it should be a robust tracer reflecting the integrated source contributions from locally emitted and transported NH_3 and pNH_4^+. Therefore, the $\delta^{15}N(NH_x)$ observations would suggest a seasonal change in sources of NH_x with increased relative emissions from a source with a high $\delta^{15}N(NH_3)$ value during the colder periods of winter and spring and a lower $\delta^{15}N(NH_3)$ value during summer. Vehicle emissions have an elevated $\delta^{15}N(NH_3)$ value of 6.6±2.1‰ (Walters et al., 2020; Song et al., 2021), such that the relative importance of vehicle emissions to NH_x in Providence, RI may have increased during colder seasons. The observed $\delta^{15}N(NH_x)$ decrease during summer and increase in $[NH_3]$ might suggest increased emissions from temperature-dependent emission sources with a relatively low $\delta^{15}N(NH_3)$ signature, such as volatilization (Felix et al., 2013; Freyer, 1978; Heaton, 1987; Chang et al., 2016; Hristov et al., 2009). There were often large $\delta^{15}N(NH_x)$ variations within each season, which may be related to wind direction shifts and varying contributions from local urban NH_3 emission sources and long-range transport of NH_x.

3.4 Identifying Urban Local Sources of NH_x

Wind data and bivariate plot statistical analysis were utilized to investigate local and transported sources of urban NH_x. The local wind data indicated a clear shift in wind direction and speed from generally faster winds from the west/northwest during winter to slower winds from the south/southeast and northeast during summer (Figure 6). Wind direction and wind speed polar bivariate CBPF plots of $[NH_3]$ and $[pNH_4^+]$ indicated relative high probability under conditions of low wind speeds (i.e., < 2 m/s) for all seasons, suggesting the importance of local emitted NH_3 sources and pNH_4^+ formation. These elevated CBPF probabilities were also associated with winds from the southeast to west, the direction of I-195 and I-95, major interstate highways, and industrial sources (Figure 1). The highest $\delta^{15}N(NH_x)$ values within each season were observed with winds from

https://doi.org/10.5194/acp-2022-419
Preprint. Discussion started: 24 June 2022


Atmospheric Chemistry and Physics Discussions

these directions, implicating the importance of vehicle emissions, which have an elevated $\delta^{15}N(NH_3)$ signature of 6.6±2.1‰ compared to other NH_3 sources that tend to have $\delta^{15}N(NH_3)$ values below 0‰, including available industrial $\delta^{15}N(NH_3)$ emissions (Walters et al., 2020).

Additionally, high CPF probabilities for both $[NH_3]$ and $[pNH_4^+]$ were observed during the warmer seasons of summer and autumn from moderate winds (2-4 m/s) from the northeast and west. This result may implicate local temperature-dependent NH_3 emission sources such as sewerage lines, trash cans, soil emissions from green spaces, and regional transport. These winds were associated with a relatively low $\delta^{15}N(NH_x)$, consistent with volatilization contributions with a low $\delta^{15}N(NH_3)$ emission signature between -56.1 to -10.3‰ based on livestock waste and fertilizer studies (Heaton, 1987; Freyer, 1978; Felix et al., 2013; Chang et al., 2016). Low CPF probabilities for both $[NH_3]$ and $[pNH_4^+]$ were generally associated with high wind speeds (i.e., > 4 m/s), reflecting the dilution of these pollutants and strong background mixing. An exception to this trend was observed for $[pNH_4^+]$ during the winter, which had elevated CPF probabilities with high wind speeds indicating the importance of long-range transport. Interestingly, there was a seasonal difference in $\delta^{15}N(NH_x)$ from this wind profile, with high values during the cold seasons and low values during summer, suggesting that the background NH_x had larger contributions from vehicle emissions and volatilization during the cold and warm seasons, respectively.

3.5 Role of Long-Range Transport as a Source of Urban NH_x

Air mass back trajectories and PSCF analysis were utilized to identify source locations of transported NH_3 and pNH_4^+ to Providence, RI. The clustered seasonal air mass back trajectories indicated a shift in the seasonal air mass origin with winds originating from the north and west during winter with higher contributions of air masses derived from the south and along the coast during summer (Figure 7). During summer and autumn, potentially significant NH_3 and pNH_4^+ source regions originated over the mid-Atlantic, midwestern US, Atlantic coast, southeastern US, southeastern Ontario, and southeastern Quebec. These regions have significant agricultural-related NH_3 emissions such as fertilizer application and livestock waste. Transport from these regions tended to have relatively low mean $\delta^{15}N(NH_x)$ values (i.e., -15 to -5‰), consistent with transport of volatilized agricultural NH_3 emissions that favor the release of isotopically light $^{14}NH_3$ (Heaton, 1987; Freyer, 1978; Felix et al., 2013; Chang et al., 2016). Indeed, available ground-based monitoring data indicates these regions tend to have elevated ambient $[NH_3]$ and $[pNH_4^+]$, consistent with these regions as potential NH_3 and pNH_4^+ source contributors to Providence, RI (Figure S3). The high CBPF probability from southeast Canada may also represent wildfire NH_3 emissions, as summer and autumn typically correspond to high wildfire activity in this region (Matz et al., 2020). Direct wildfire $\delta^{15}N(NH_3)$ emission signatures are unknown; however, emissions from biomass burning (coal combustion) report an emission signature of -6.1±1.3‰ (Freyer, 1978), which is within the range of values observed from the potentially contributing biomass burning regions. Additionally, the Atlantic coast may represent contributions from ocean NH_3 flux, which has been suggested to have low $\delta^{15}N$ values (Jickells et al., 2003).

https://doi.org/10.5194/acp-2022-419
Preprint. Discussion started: 24 June 2022


Atmospheric Chemistry and Physics Discussions

Elevated PSCF probabilities were identified for [pNH_4^+] during the winter from the mid-Atlantic and Midwestern US, which is consistent with available [pNH_4^+] ground-based observations that tend to peak during this period due to ambient conditions that favor the formation of NH_4NO_3 (Figure S3). This transport region tended to have relatively high mean $\delta^{15}N(NH_x)$ values (e.g., -5 to 0‰) from the Midwestern US and relatively low mean from the Mid-Atlantic (~-10‰). Across the US, [NH_3] was lowest during winter due to decreased agricultural activities (Figure S3). Indeed, the NEI-14 indicates that the relative importance of non-agricultural NH_3 sources increases during winter (Figure 4), such that the higher $\delta^{15}N(NH_x)$ values deriving from the Midwest may reflect the regional importance of sources with an elevated $\delta^{15}N(NH_3)$ value such as vehicles and/or fuel-combustion. Lower mean $\delta^{15}N(NH_x)$ values derived from the mid-Atlantic may suggest that agricultural emissions such as animal housing remain an important wintertime NH_x source contributor to Providence, RI. Additionally, there could be contributions from fuel combustion with selective catalytic reduction technology that have a reported $\delta^{15}N(NH_3)$ signature of -14.6 to -11.3‰ (Felix et al., 2013).

3.5 Urban NH_x Source Apportionment

The NH_x source contributions at Providence, RI, including local and transported emissions, were quantified using SIMMR (Parnell et al., 2010). The model was initiated using the measured $\delta^{15}N(NH_x)$ values and assuming vehicles, volatilization, fuel combustion with selective catalytic converters (SCR), industry, and biomass burning were the main sources, as evidenced by the local wind direction and back trajectory analysis and the NEI-14 predictions. We acknowledge that there are additional miscellaneous NH_3 sources in an urban environment, including pets, household products, and humans; however, we assumed that these sources were negligible compared to the main identified emission sources.

The source apportionment results are sensitive to the number of considered sources, their designated $\delta^{15}N(NH_3)$ emission signatures, and uncertainty. The input $\delta^{15}N(NH_3)$ emission source signatures were deliberately chosen from sampling methodologies that have utilized active sampling approaches, as it has been well-documented from several studies that passive samplers result in a $\delta^{15}N(NH_3)$ bias and could be unreliable (Pan et al., 2020; Kawashima et al., 2021; Walters et al., 2020). Fertilization application is a significant source of NH_3 emissions globally and within the US. However, fertilizer application represents a small component of the overall agricultural emissions at our site (~1.8%) and within our region (7.1%; US EPA Region 1) based on the NEI-14. Further, fertilization-related NH_3 emissions tend to peak during spring; however, we neither identified any significant NH_x long-range transport region nor observed a relative decrease in $\delta^{15}N(NH_x)$ during spring, which would be consistent with a suspected low fertilizer volatilization $\delta^{15}N(NH_3)$ emission signature. Thus, fertilizer application was not considered in our source apportionment model.

https://doi.org/10.5194/acp-2022-419
Preprint. Discussion started: 24 June 2022


Atmospheric Chemistry and Physics Discussions

The input source values for vehicles, fuel combustion (SCR)/industry, biomass burning/coal, and volatilization were fixed at 6.6±2.1‰ (Walters et al., 2020), -15.3±3.6‰ (Heaton, 1987; Freyer, 1978), -6.1±1.3‰ (Freyer, 1978), and -19.2±8.3‰ (Freyer, 1978; Heaton, 1987; Hristov et al., 2009; Frank et al., 2004). Fuel combustion with SCR and industry $\delta^{15}N(NH_3)$ emission signature was grouped due to similar values. The volatilization $\delta^{15}N(NH_3)$ emission signature represents integrated volatilization measurements conducted in animal sheds (Freyer, 1978; Heaton, 1987), and measurements that include monitoring volatilization as a function of time, which indicate significant $\delta^{15}N(NH_3)$ variability (Hristov et al., 2009; Frank et al., 2004). Further details on our rationale for the chosen source $\delta^{15}N$ values are provided in the Supporting Information (Text S1).

The mixing model predicts that vehicles, volatilization, fuel-combustion (SCR)/industry, and biomass/coal contribute (mean±σ) 30.7±11.6%, 17.0±10.8%, 18.3±12.1%, and 33.9±23.4% to the annual NH_x background in Providence, RI (Figure 8). The relative contribution of vehicle emissions had a strong seasonal profile with higher contributions during the colder seasons of spring (42.9±11.3%) and winter (45.8±13.0%) compared to the warmer seasons of summer (20.8±9.7%) and autumn (29.5±12.2%). The relative contribution for volatilization and fuel combustion (SCR)/industry was predicted to peak during summer with means of 24.9±13.8% and 24.8±15.9%, compared to winter with means of 14.1±8.7%, 15.1±10.0%, respectively. Biomass/coal emissions were relatively consistent across seasons, with a peak during autumn of 33.3±22.6%.

The input emission signatures for volatilization and fuel combustion (SCR)/industry have somewhat overlapping values, such that it was difficult for the mixing model to differentiate between these sources. Based on the NEI-14, wind direction, and long-range transport analysis (Figures 4, 6, & 7), we suspect the relative contribution of vehicle emissions diminished during summer due to the importance of temperature-dependent NH_3 volatilization emissions. The exact NH_3 volatilization source remains unclear. There was evidence of significant contributions from local urban volatilization (i.e., sewage, waste, urban green spaces) and long-range transport from regional agricultural activities and ocean flux (Figures 6 and 7). Stationary fuel combustion and industry NH_3 emissions were unlikely to explain the seasonal shift in the relative increase of non-vehicle emissions observed during summer, as the NEI-14 predicts stationary fuel combustion emissions as more important contributors during winter due to significant heating demand, and industrial emissions were expected to have a non-seasonally dependent emission profile (Figure 4). Interestingly, a relatively low fractional contribution was predicted for fuel combustion (SCR) for winter, despite the NEI-14 indicating that residential fuel (natural gas and oil) combustion was the largest emission source of NH_3 at our study site and other cities with significant heating demands (Zhou et al., 2019). While we acknowledge that the fuel combustion $\delta^{15}N(NH_3)$ emission signatures were uncertain, the mixing model and seasonal $[NH_3]$ results would suggest that residential NH_3 emissions were overpredicted in the NEI. Their emission factors may need to be revisited to more accurately model urban $[NH_3]$ and predict its human and ecological impacts. Biomass burning could be a seasonal consistent contributing NH_x source due to the role of residential wood combustion (Figure 4) during colder months and wildfires during the warmer months. However, the $\delta^{15}N$ source apportionment results for biomass burning predict an extremely broad

https://doi.org/10.5194/acp-2022-419
Preprint. Discussion started: 24 June 2022


Atmospheric Chemistry and Physics Discussions

425 distribution (Figure 8; Figure S4). Future NH_x source apportionment of biomass burning should consider additional biomass tracers such as potassium and levoglucosan.

4. Conclusion

Elevated urban NH_x concentrations were observed in Providence, RI, relative to regional background monitoring stations in New England. Mixing model $\delta^{15}N(NH_x)$ source apportionment results utilizing $\delta^{15}N(NH_x)$, suggest that vehicles represent an
430 important source of urban NH_x with strong seasonal variability. The relative contribution of vehicle emissions was highest during winter/spring, which is significant because NH_3 emissions may contribute to the elevated $PM_{2.5}$ observed during this time in the eastern US (Shah et al., 2018). Reductions in vehicle ammonia emissions may represent a promising way to mitigate the adverse impacts of elevated urban NH_3 concentrations and yield positive benefits for ecosystems and human health. However, vehicle NH_3 emissions are a consequence of the technology used to combat vehicle NO_x and CO emissions.
435 Decreasing vehicle NH_3 emissions may not be achievable until the vehicle fleet electrification. Expanding national observational networks to include urban measurements of $[NH_3]$ and $\delta^{15}N(NH_x)$ are needed to monitor urban trends and design future regulatory NH_3 fossil-fuel-related emission reductions.

This work demonstrated that nitrogen isotopic analysis allows for further refinement of our understanding and quantification
440 of urban NH_x sources, laying the foundation for future source apportionment studies. Utilizing a laboratory-verified collection method suitable for NH_x speciation and isotope analysis was critical for accurate source apportionment due to the observed complex phase-dependent $\delta^{15}N$ isotope fractionation between NH_3 and pNH_4^+. Future studies should improve our understanding of the drivers behind NH_3 and pNH_4^+ phase $\delta^{15}N$ fractionation, including controlled chamber studies and field observations, which may also provide important insights into controls on NH_3/pNH_4^+ gas to particle-phase conversion. Still,
445 this work highlights the need to improve our $\delta^{15}N(NH_3)$ emission source values, particularly for our volatilization, industry, fuel combustion, and biomass burning sources, to enhance the quality of the source apportionment results.

Data Availability. Data presented in this article are available on the Harvard Dataeverse at
450 https://doi.org/10.7910/DVN/JHMBRI and in the Supplement .

Author contributions. WWW, MK, and MGH designed varying aspects of the field sampling plan. WWW, MK, and DEB carried out the field measurements. WWW, MK, and DEB conducted all laboratory analyses of data. EW contributed spatial analysis of data. BHB contributed emission modelling of the presented data. WWW prepared the article with contributions
455 from all co-authors.

https://doi.org/10.5194/acp-2022-419
Preprint. Discussion started: 24 June 2022

Atmospheric Chemistry and Physics Discussions

Competing interests. The authors declare that they have no conflict of interest.

Acknowledgements. We thank Ruby Ho for sampling and laboratory assistance. We are grateful to Paul Theroux of RI-DEM/RI-DOH for access and support at the RI-DEM air-monitoring sites.

Financial support. This research has been supported by the National Science Foundation Division of Atmospheric and Geospace Sciences (grant: 1624618) and the Institute at Brown for Environment and Society (internal grant no. GR300123).

References

Ashbaugh, L. L. and Eldred, R. A.: Loss of particle nitrate from teflon sampling filters: effects on measured gravimetric mass in California and in the IMPROVE network, J. Air Waste Manag. Assoc. 1995, 54, 93–104, 2004.

Baek, B. H. and Seppanen, C.: CEMPD/SMOKE: SMOKE v4.8.1 Public Release (January 29, 2021), 2021.

Begum, B. A., Kim, E., Jeong, C.-H., Lee, D.-W., and Hopke, P. K.: Evaluation of the potential source contribution function using the 2002 Quebec forest fire episode, Atmos. Environ., 39, 3719–3724, 2005.

Behera, S. N. and Sharma, M.: Investigating the potential role of ammonia in ion chemistry of fine particulate matter formation for an urban environment, Sci. Total Environ., 408, 3569–3575, 2010.

Behera, S. N., Sharma, M., Aneja, V. P., and Balasubramanian, R.: Ammonia in the atmosphere: a review on emission sources, atmospheric chemistry and deposition on terrestrial bodies, Environ. Sci. Pollut. Res., 20, 8092–8131, 2013.

Berner, A. H. and David Felix, J.: Investigating ammonia emissions in a coastal urban airshed using stable isotope techniques, Sci. Total Environ., 707, 134952, 2020.

Bhattarai, N., Wang, S., Xu, Q., Dong, Z., Chang, X., Jiang, Y., and Zheng, H.: Sources of gaseous NH3 in urban Beijing from parallel sampling of NH3 and NH4+, their nitrogen isotope measurement and modeling, Sci. Total Environ., 747, 141361, 2020.

Bhattarai, N., Wang, S., Pan, Y., Xu, Q., Zhang, Y., Chang, Y., and Fang, Y.: δ15N-stable isotope analysis of NHx: An overview on analytical measurements, source sampling and its source apportionment, Front. Environ. Sci. Eng., 15, 126, 2021.

https://doi.org/10.5194/acp-2022-419
Preprint. Discussion started: 24 June 2022

Böhlke, J. K. and Coplen, T. B.: Reference and intercomparison materials for stable isotopes of light elements, in: Proceedings of the IAEA-TECDOC-825 Consultants Meeting Held in Vienna, Vienna, Austria, 1993.

Bohlke, J. k., Gwinn, C. j., and Coplen, T. b.: New Reference Materials for Nitrogen-Isotope-Ratio Measurements, Geostand. Newsl., 17, 159–164, 1993.

Böhlke, J. K., Smith, R. L., and Hannon, J. E.: Isotopic analysis of N and O in nitrite and nitrate by sequential selective bacterial reduction to N2O, Anal. Chem., 79, 5888–5895, 2007.

Bouwman, A. F., Lee, D. S., Asman, W. A. H., Dentener, F. J., Van Der Hoek, K. W., and Olivier, J. G. J.: A global high-resolution emission inventory for ammonia, Glob. Biogeochem. Cycles, 11, 561–587, 1997.

Cao, H., Henze, D. K., Cady-Pereira, K., McDonald, B. C., Harkins, C., Sun, K., Bowman, K. W., Fu, T.-M., and Nawaz, M. O.: COVID-19 Lockdowns Afford the First Satellite-Based Confirmation That Vehicles Are an Under-recognized Source of Urban NH3 Pollution in Los Angeles, Environ. Sci. Technol. Lett., 2021.

Carslaw, D. C. and Ropkins, K.: Openair—an R package for air quality data analysis, Environ. Model. Softw., 27, 52–61, 2012.

Carslaw, D. C., Beevers, S. D., Ropkins, K., and Bell, M. C.: Detecting and quantifying aircraft and other on-airport contributions to ambient nitrogen oxides in the vicinity of a large international airport, Atmos. Environ., 40, 5424–5434, 2006.

Cass, G. R., Gharib, S., Peterson, M., and Tilden, J. W.: The origin of ammonia emissions to the atmosphere in an urban area, Open File Rep., 82–6, 1982.

Chang, Y., Liu, X., Deng, C., Dore, A. J., and Zhuang, G.: Source apportionment of atmospheric ammonia before, during, and after the 2014 APEC summit in Beijing using stable nitrogen isotope signatures, Atmospheric Chem. Phys., 16, 11635–11647, 2016.

Crittenden, P. D., Scrimgeour, C. M., Minnullina, G., Sutton, M. A., Tang, Y. S., and Theobald, M. R.: Lichen response to ammonia deposition defines the footprint of a penguin rookery, Biogeochemistry, 122, 295–311, 2015.

https://doi.org/10.5194/acp-2022-419
Preprint. Discussion started: 24 June 2022


Atmospheric Chemistry and Physics Discussions

520 Decina, S. M., Templer, P. H., Hutyra, L. R., Gately, C. K., and Rao, P.: Variability, drivers, and effects of atmospheric nitrogen inputs across an urban area: emerging patterns among human activities, the atmosphere, and soils, Sci. Total Environ., 609, 1524–1534, 2017.

Decina, S. M., Hutyra, L. R., and Templer, P. H.: Hotspots of nitrogen deposition in the world's urban areas: a global data
525 synthesis, Front. Ecol. Environ., 18, 92–100, 2020.

Felix, D. J., Elliott, E. M., Gish, T. J., McConnell, L. L., and Shaw, S. L.: Characterizing the isotopic composition of atmospheric ammonia emission sources using passive samplers and a combined oxidation-bacterial denitrifier approach, Rapid Commun. Mass Spectrom., 27, 2239–2246, 2013.

530

Felix, J. D., Elliott, E. M., and Gay, D. A.: Spatial and temporal patterns of nitrogen isotopic composition of ammonia at US ammonia monitoring network sites, Atmos. Environ., 150, 434–442, 2017.

Fenn, M. E., Bytnerowicz, A., Schilling, S. L., Vallano, D. M., Zavaleta, E. S., Weiss, S. B., Morozumi, C., Geiser, L. H., and
535 Hanks, K.: On-road emissions of ammonia: An underappreciated source of atmospheric nitrogen deposition, Sci. Total Environ., 625, 909–919, 2018.

Fleming, Z. L., Monks, P. S., and Manning, A. J.: Untangling the influence of air-mass history in interpreting observed atmospheric composition, Atmospheric Res., 104, 1–39, 2012.

540

Frank, D. A., Evans, R. D., and Tracy, B. F.: The role of ammonia volatilization in controlling the natural 15N abundance of a grazed grassland, Biogeochemistry, 68, 169–178, 2004.

Freyer, H. D.: Seasonal trends of NH4+ and NO3- nitrogen isotope composition in rain collected at Jülich, Germany, Tellus,
545 30, 83–92, 1978.

Galloway, J. N., Dentener, F. J., Capone, D. G., Boyer, E. W., Howarth, R. W., Seitzinger, S. P., Asner, G. P., Cleveland, C., Green, P., and Holland, E.: Nitrogen cycles: past, present, and future, Biogeochemistry, 70, 153–226, 2004.

550 Heaton, T. H. E.: 15N14N ratios of nitrate and ammonium in rain at Pretoria, South Africa, Atmospheric Environ. 1967, 21, 843–852, 1987.

https://doi.org/10.5194/acp-2022-419
Preprint. Discussion started: 24 June 2022

Hristov, A. N., Zaman, S., Vander Pol, M., Ndegwa, P., Campbell, L., and Silva, S.: Nitrogen losses from dairy manure estimated through nitrogen mass balance and chemical markers, J. Environ. Qual., 38, 2438–2448, 2009.

Hu, Q., Zhang, L., Evans, G. J., and Yao, X.: Variability of atmospheric ammonia related to potential emission sources in downtown Toronto, Canada, Atmos. Environ., 99, 365–373, 2014.

Jickells, T. D., Kelly, S. D., Baker, A. R., Biswas, K., Dennis, P. F., Spokes, L. J., Witt, M., and Yeatman, S. G.: Isotopic evidence for a marine ammonia source, Geophys. Res. Lett., 30, 1374, 2003.

Joyce, E. E., Walters, W. W., Roy, E. L., Clark, S. C., Schiebel, H., and Hastings, M. G.: Highly concentrated atmospheric inorganic nitrogen deposition in an urban, coastal region in the US, Environ. Res. Commun., 2, 081001, 2020.

Kawashima, H. and Ono, S.: Nitrogen Isotope Fractionation from Ammonia Gas to Ammonium in Particulate Ammonium Chloride, Environ. Sci. Technol., 53, 10629–10635, 2019.

Kawashima, H., Ogata, R., and Gunji, T.: Laboratory-based validation of a passive sampler for determination of the nitrogen stable isotope ratio of ammonia gas, Atmos. Environ., 245, 118009, 2021.

Koutrakis, P., Wolfson, J. M., and Spengler, J. D.: An improved method for measuring aerosol strong acidity: results from a nine-month study in St Louis, Missouri and Kingston, Tennessee, Atmospheric Environ. 1967, 22, 157–162, 1988.

Koutrakis, P., Sioutas, C., Ferguson, S. T., Wolfson, J. M., Mulik, J. D., and Burton, R. M.: Development and evaluation of a glass honeycomb denuder/filter pack system to collect atmospheric gases and particles, Environ. Sci. Technol., 27, 2497–2501, 1993.

Liu, J., Ding, P., Zong, Z., Li, J., Tian, C., Chen, W., Chang, M., Salazar, G., Shen, C., and Cheng, Z.: Evidence of rural and suburban sources of urban haze formation in China: a case study from the Pearl River Delta region, J. Geophys. Res. Atmospheres, 123, 4712–4726, 2018.

Matz, C. J., Egyed, M., Xi, G., Racine, J., Pavlovic, R., Rittmaster, R., Henderson, S. B., and Stieb, D. M.: Health impact analysis of PM2.5 from wildfire smoke in Canada (2013–2015, 2017–2018), Sci. Total Environ., 725, 138506, 2020.

McIlvin, M. R. and Altabet, M. A.: Chemical Conversion of Nitrate and Nitrite to Nitrous Oxide for Nitrogen and Oxygen Isotopic Analysis in Freshwater and Seawater, Anal. Chem., 77, 5589–5595, 2005.

https://doi.org/10.5194/acp-2022-419
Preprint. Discussion started: 24 June 2022


Atmospheric Chemistry and Physics Discussions

Meng, Z. and Seinfeld, J. H.: Time scales to achieve atmospheric gas-aerosol equilibrium for volatile species, Atmos. Environ., 30, 2889–2900, 1996.

Meng, Z. Y., Lin, W. L., Jiang, X. M., Yan, P., Wang, Y., Zhang, Y. M., Jia, X. F., and Yu, X. L.: Characteristics of atmospheric ammonia over Beijing, China, Atmospheric Chem. Phys., 11, 6139–6151, 2011.

Muzio, L. J. and Arand, J. K.: Homogeneous Gas Phase Decomposition of Oxides of Nitrogen. Tustin, CA, KVB Incorporated, Electr. Power Res. Inst. Rep. FP-253 Proj., 461, 1976.

Nowak, J. B., Huey, L. G., Russell, A. G., Tian, D., Neuman, J. A., Orsini, D., Sjostedt, S. J., Sullivan, A. P., Tanner, D. J., Weber, R. J., and others: Analysis of urban gas phase ammonia measurements from the 2002 Atlanta Aerosol Nucleation and Real-Time Characterization Experiment (ANARChE), J. Geophys. Res. Atmospheres 1984–2012, 111, 2006.

Pan, Y., Tian, S., Liu, D., Fang, Y., Zhu, X., Zhang, Q., Zheng, B., Michalski, G., and Wang, Y.: Fossil Fuel Combustion-Related Emissions Dominate Atmospheric Ammonia Sources during Severe Haze Episodes: Evidence from 15N-Stable Isotope in Size-Resolved Aerosol Ammonium, Environ. Sci. Technol., 50, 8049–8056, 2016.

Pan, Y., Tian, S., Liu, D., Fang, Y., Zhu, X., Gao, M., Gao, J., Michalski, G., and Wang, Y.: Isotopic evidence for enhanced fossil fuel sources of aerosol ammonium in the urban atmosphere, Environ. Pollut., 238, 942–947, 2018.

Pan, Y., Gu, M., Song, L., Tian, S., Wu, D., Walters, W. W., Yu, X., Lü, X., Ni, X., and Wang, Y.: Systematic low bias of passive samplers in characterizing nitrogen isotopic composition of atmospheric ammonia, Atmospheric Res., 105018, 2020.

Parnell, A. C., Inger, R., Bearhop, S., and Jackson, A. L.: Source partitioning using stable isotopes: coping with too much variation, PloS One, 5, e9672, 2010.

Paulot, F., Ginoux, P., Cooke, W. F., Donner, L. J., Fan, S., Lin, M.-Y., Mao, J., Naik, V., and Horowitz, L. W.: Sensitivity of nitrate aerosols to ammonia emissions and to nitrate chemistry: implications for present and future nitrate optical depth, Atmospheric Chem. Phys., 16, 1459–1477, 2016.

Pekney, N. J., Davidson, C. I., Zhou, L., and Hopke, P. K.: Application of PSCF and CPF to PMF-modeled sources of PM2. 5 in Pittsburgh, Aerosol Sci. Technol., 40, 952–961, 2006.

Plautz, J.: Piercing the haze, Science, 361, 1060–1063, 2018.

https://doi.org/10.5194/acp-2022-419
Preprint. Discussion started: 24 June 2022


Atmospheric Chemistry and Physics Discussions

Puchalski, M. A., Rogers, C. M., Baumgardner, R., Mishoe, K. P., Price, G., Smith, M. J., Watkins, N., and Lehmann, C. M.: A statistical comparison of active and passive ammonia measurements collected at Clean Air Status and Trends Network (CASTNET) sites, Environ. Sci. Process. Impacts, 17, 358–369, 2015.

Savard, M. M., Cole, A., Smirnoff, A., and Vet, R.: δ15N values of atmospheric N species simultaneously collected using sector-based samplers distant from sources – Isotopic inheritance and fractionation, Atmos. Environ., 162, 11–22, 2017.

Shah, V., Jaeglé, L., Thornton, J. A., Lopez-Hilfiker, F. D., Lee, B. H., Schroder, J. C., Campuzano-Jost, P., Jimenez, J. L., Guo, H., Sullivan, A. P., Weber, R. J., Green, J. R., Fiddler, M. N., Bililign, S., Campos, T. L., Stell, M., Weinheimer, A. J., Montzka, D. D., and Brown, S. S.: Chemical feedbacks weaken the wintertime response of particulate sulfate and nitrate to emissions reductions over the eastern United States, Proc. Natl. Acad. Sci., 115, 8110–8115, 2018.

Skinner, R., Ineson, P., Jones, H., Sleep, D., and Theobald, M.: Sampling systems for isotope-ratio mass spectrometry of atmospheric ammonia, Rapid Commun. Mass Spectrom., 20, 81–88, 2006.

Song, L., Walters, W. W., Pan, Y., Li, Z., Gu, M., Duan, Y., Lü, X., and Fang, Y.: 15N natural abundance of vehicular exhaust ammonia, quantified by active sampling techniques, Atmos. Environ., 255, 118430, 2021.

Stein, A. F., Draxler, R. R., Rolph, G. D., Stunder, B. J., Cohen, M. D., and Ngan, F.: NOAA's HYSPLIT atmospheric transport and dispersion modeling system, Bull. Am. Meteorol. Soc., 96, 2059–2077, 2015.

Suarez-Bertoa, R., Zardini, A. A., and Astorga, C.: Ammonia exhaust emissions from spark ignition vehicles over the New European Driving Cycle, Atmos. Environ., 97, 43–53, 2014.

Suarez-Bertoa, R., Mendoza-Villafuerte, P., Riccobono, F., Vojtisek, M., Pechout, M., Perujo, A., and Astorga, C.: On-road measurement of NH3 emissions from gasoline and diesel passenger cars during real world driving conditions, Atmos. Environ., 166, 488–497, 2017.

Sun, K., Tao, L., Miller, D. J., Khan, M. A., and Zondlo, M. A.: On-Road Ammonia Emissions Characterized by Mobile, Open-Path Measurements, Environ. Sci. Technol., 48, 3943–3950, 2014.

Sun, K., Tao, L., Miller, D. J., Pan, D., Golston, L. M., Zondlo, M. A., Griffin, R. J., Wallace, H. W., Leong, Y. J., Yang, M. M., Zhang, Y., Mauzerall, D. L., and Zhu, T.: Vehicle Emissions as an Important Urban Ammonia Source in the United States and China, Environ. Sci. Technol., 51, 2472–2481, 2017.

https://doi.org/10.5194/acp-2022-419
Preprint. Discussion started: 24 June 2022

655 Tomlin, A. S., Smalley, R. J., Tate, J. E., Barlow, J. F., Belcher, S. E., Arnold, S. J., Dobre, A., and Robins, A.: A field study of factors influencing the concentrations of a traffic-related pollutant in the vicinity of a complex urban junction, Atmos. Environ., 43, 5027–5037, 2009.

Updyke, K. M., Nguyen, T. B., and Nizkorodov, S. A.: Formation of brown carbon via reactions of ammonia with secondary
660 organic aerosols from biogenic and anthropogenic precursors, Atmos. Environ., 63, 22–31, 2012.

Urey, H. C.: The thermodynamic properties of isotopic substances, J Chem Soc, 7, 562–581, 1947.

Uria-Tellaetxe, I. and Carslaw, D. C.: Conditional bivariate probability function for source identification, Environ. Model.
665 Softw., 59, 1–9, 2014.

Van Damme, M., Clarisse, L., Whitburn, S., Hadji-Lazaro, J., Hurtmans, D., Clerbaux, C., and Coheur, P.-F.: Industrial and agricultural ammonia point sources exposed, Nature, 564, 99, 2018.

670 Walker, J. T., Whitall, D. R., Robarge, W., and Paerl, H. W.: Ambient ammonia and ammonium aerosol across a region of variable ammonia emission density, Atmos. Environ., 38, 1235–1246, 2004.

Walters, W. W. and Hastings, M. G.: Collection of Ammonia for High Time-Resolved Nitrogen Isotopic Characterization Utilizing an Acid-Coated Honeycomb Denuder, Anal. Chem., 90, 8051–8057, 2018.
675

Walters, W. W., Chai, J., and Hastings, M. G.: Theoretical Phase Resolved Ammonia–Ammonium Nitrogen Equilibrium Isotope Exchange Fractionations: Applications for Tracking Atmospheric Ammonia Gas-to-Particle Conversion, ACS Earth Space Chem., 2018.

680 Walters, W. W., Blum, D. E., and Hastings, M. G.: Selective Collection of Particulate Ammonium for Nitrogen Isotopic Characterization Using a Denuder–Filter Pack Sampling Device, Anal. Chem., 2019.

Walters, W. W., Song, L., Chai, J., Fang, Y., Colombi, N., and Hastings, M. G.: Characterizing the spatiotemporal nitrogen stable isotopic composition of ammonia in vehicle plumes, Atmospheric Chem. Phys., 20, 11551–11567, 2020a.
685

Walters, W. W., Song, L., Chai, J., Fang, Y., Colombi, N., and Hastings, M. G.: Constraining Ammonia Emissions in Vehicle Plumes Utilizing Nitrogen Stable Isotopes, Atmospheric Chem. Phys. Discuss., 1–48, 2020b.

Wang, S., Nan, J., Shi, C., Fu, Q., Gao, S., Wang, D., Cui, H., Saiz-Lopez, A., and Zhou, B.: Atmospheric ammonia and its impacts on regional air quality over the megacity of Shanghai, China, Sci. Rep., 5, 15842, 2015.

Wu, L., Ren, H., Wang, P., Chen, J., Fang, Y., Hu, W., Ren, L., Deng, J., Song, Y., and Li, J.: Aerosol ammonium in the urban boundary layer in Beijing: insights from nitrogen isotope ratios and simulations in summer 2015, Environ. Sci. Technol. Lett., 6, 389–395, 2019.

Xiao, H.-W., Wu, J.-F., Luo, L., Liu, C., Xie, Y.-J., and Xiao, H.-Y.: Enhanced biomass burning as a source of aerosol ammonium over cities in central China in autumn, Environ. Pollut., 266, 115278, 2020.

Yao, X. and Zhang, L.: Trends in atmospheric ammonia at urban, rural, and remote sites across North America, Atmospheric Chem. Phys., 16, 11465–11475, https://doi.org/10.5194/acp-16-11465-2016, 2016.

Yao, X., Hu, Q., Zhang, L., Evans, G. J., Godri, K. J., and Ng, A. C.: Is vehicular emission a significant contributor to ammonia in the urban atmosphere?, Atmos. Environ., 80, 499–506, 2013.

Yu, X.-Y., Lee, T., Ayres, B., Kreidenweis, S. M., Jr, J. L. C., and Malm, W.: Particulate Nitrate Measurement Using Nylon Filters, J. Air Waste Manag. Assoc., 55, 1100–1110, 2005.

https://doi.org/10.5194/acp-2022-419
Preprint. Discussion started: 24 June 2022

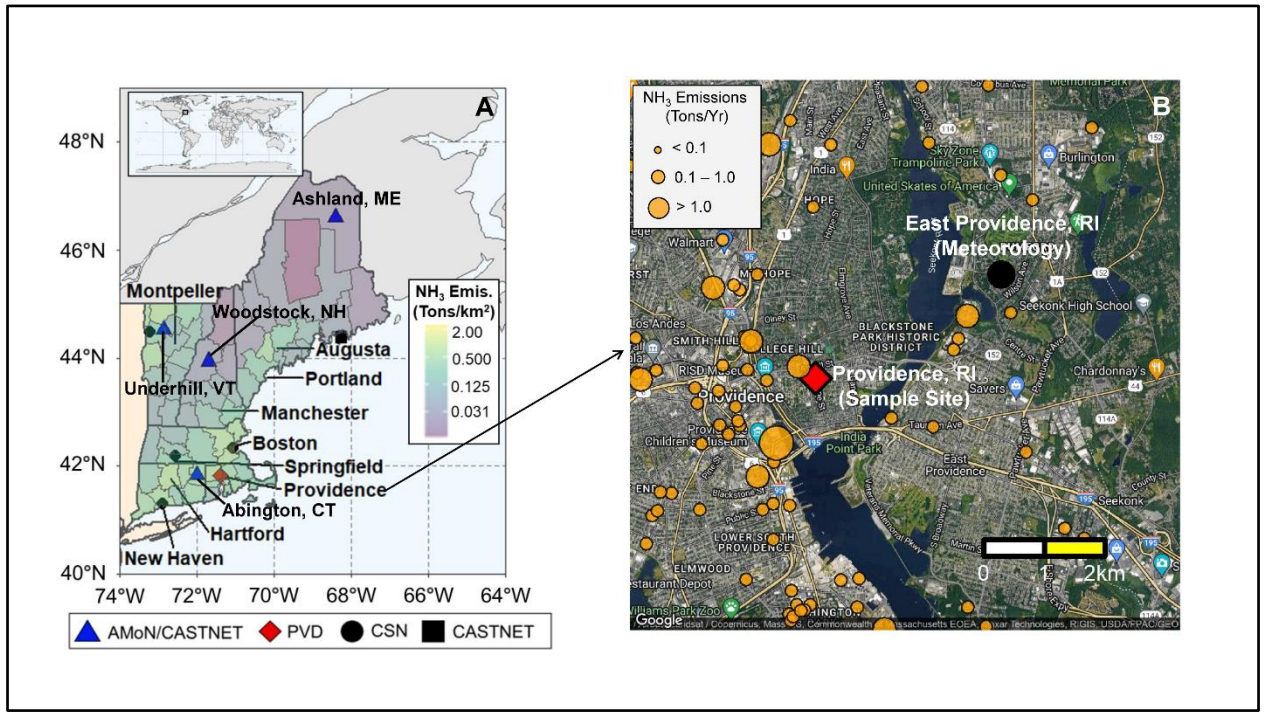

Figure 1. Overview of the sampling location in Providence, RI, USA (red diamond) located within New England (A) with the Ammonia Monitoring Network (AMoN)/Clean Air Status and Trends Network (CASTNET; blue triangle), Chemical Speciation Network (CSN; black circle), CASTNET only (black square) monitoring locations indicated. The counties in A are color-coded for NEI-14 NH_3 emission densities. The zoomed-in map of Providence, RI, US is shown in B with the sample site location (red diamond), the nearby CSN location with reported meteorology data (black circle) in East Providence, RI, USA, and the NH_3 point emission sources from the NEI (orange circles; size-coded to annual NH_3 emission) indicated. Image (B) was created using © Google Maps (Map data ©2019 Google).

https://doi.org/10.5194/acp-2022-419
Preprint. Discussion started: 24 June 2022

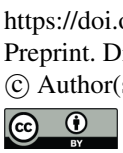

Atmospheric Chemistry and Physics Discussions

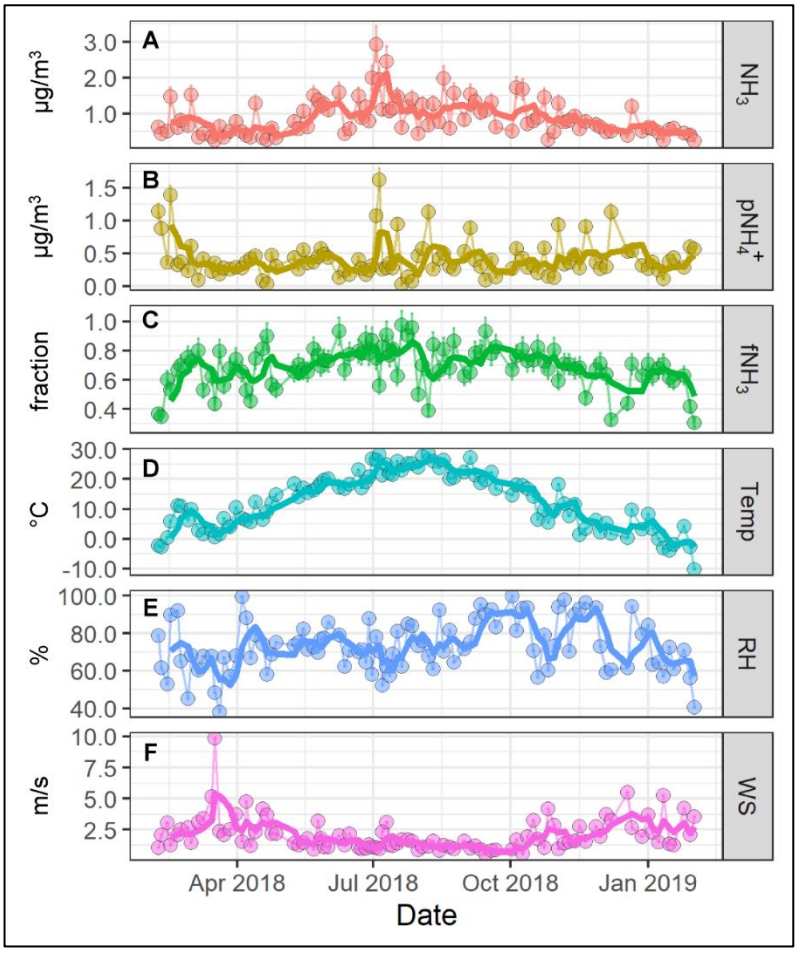

Figure 2. Time series plots of the measured NH_x data including (A) [NH_3], (B) [pNH_4^+], and (C) fNH_3 and the reported meteorology data including (C) temperature (Temp), relative humidity (RH), and wind speed (WS) from Feb 2018 – Feb 2019 in Providence, RI, US. The light data points refer to the 24-h integrated samples (A, B, C) or 24-h averaged meteorology data (D, E, F), and the dark lines represent approximate 2-week moving averages.

https://doi.org/10.5194/acp-2022-419
Preprint. Discussion started: 24 June 2022

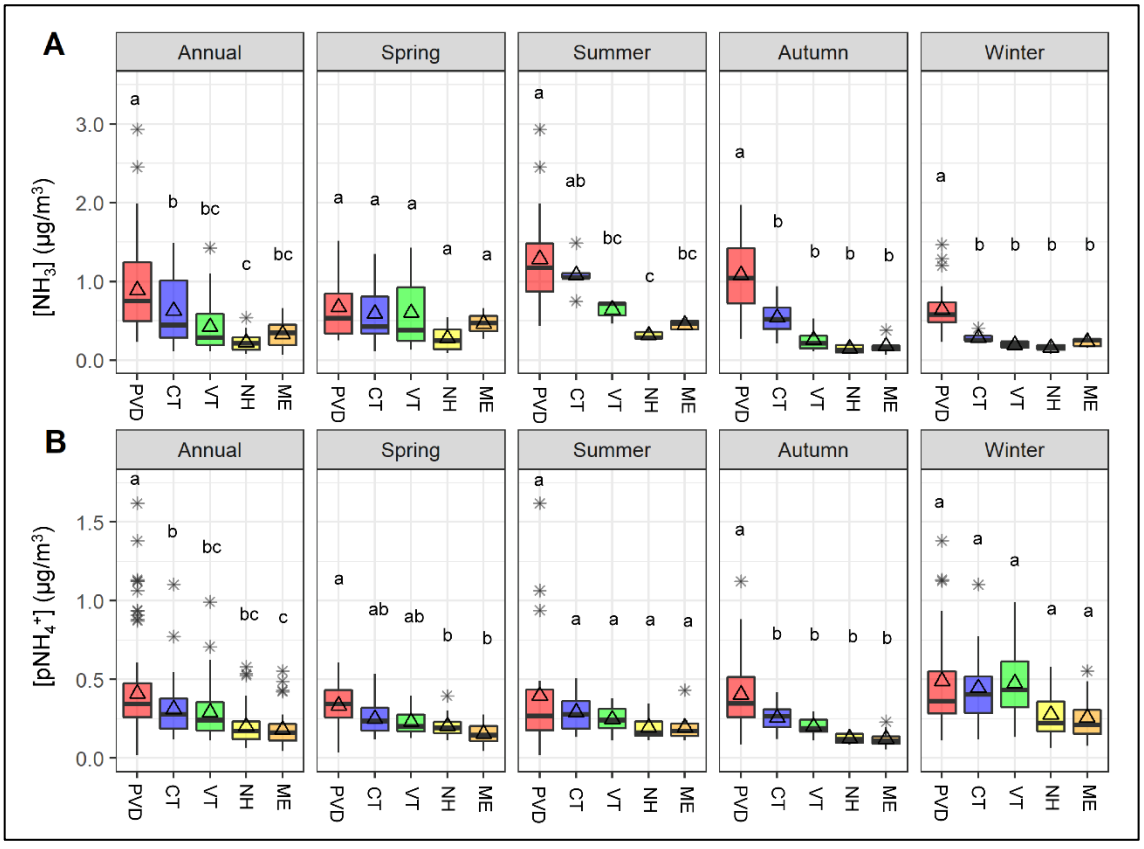

Figure 3. Box and whiskers plots that summarize the annual and seasonal (A) [NH_3] and (B) [pNH_4^+] distributions (lower extreme, lower quartile, median, upper quartile, and upper extreme) with the mean (open triangle) and outlier (black asterisk) at the Providence, RI (PVD) site and the New England AMoN/CASTNET sites including Abington, CT (CT), Underhill, VT (VT), Woodstock, NH (NH), and Ashland, ME (ME). Similar lowercase letters in the box and whiskers plots represent categories with statistically similar values.

https://doi.org/10.5194/acp-2022-419
Preprint. Discussion started: 24 June 2022

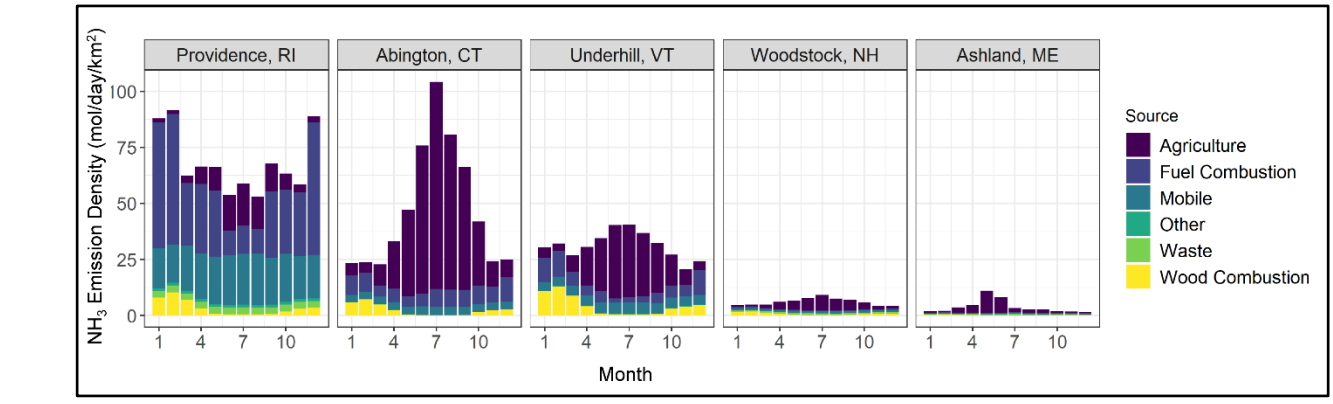

765

Figure 4. Monthly-based NH_3 emission densities speciated between agricultural, fuel combustion, mobile, other, waste, and wood combustion computed by the SMOKE model for the counties of the New England NH_3 monitoring site.

770

775

780

785

https://doi.org/10.5194/acp-2022-419
Preprint. Discussion started: 24 June 2022

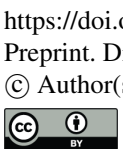

Atmospheric Chemistry and Physics Discussions

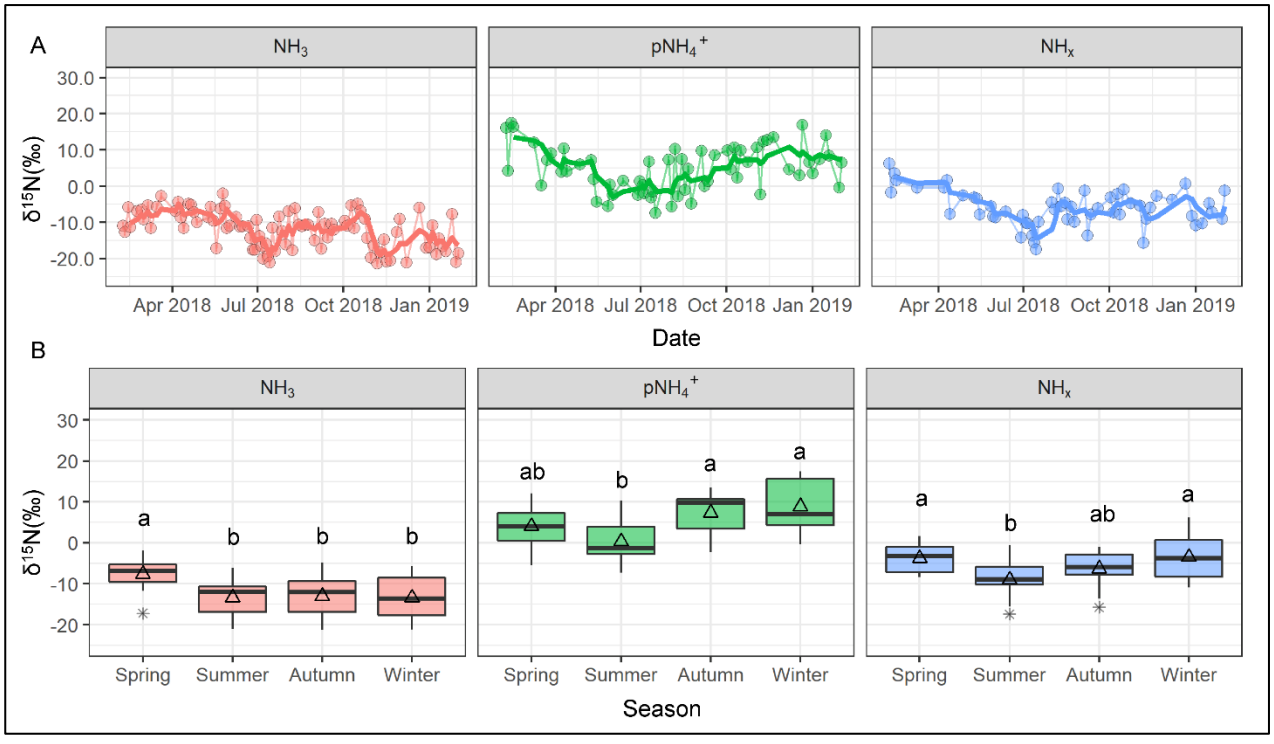

790

Figure 5. Measured $\delta^{15}N$ data of NH_3, pNH_4^+, and NH_x collected in Providence, RI, including (A) time series and (B) seasonal box and whiskers plots summarizing the distributions (lower extreme, lower quartile, median, upper quartile, and upper extreme) with the mean (open triangle) and outlier (black asterisk). Similar lowercase letters in the box and whiskers plots represent categories with statistically similar values.

795

800

805

https://doi.org/10.5194/acp-2022-419
Preprint. Discussion started: 24 June 2022

Atmospheric Chemistry and Physics Discussions

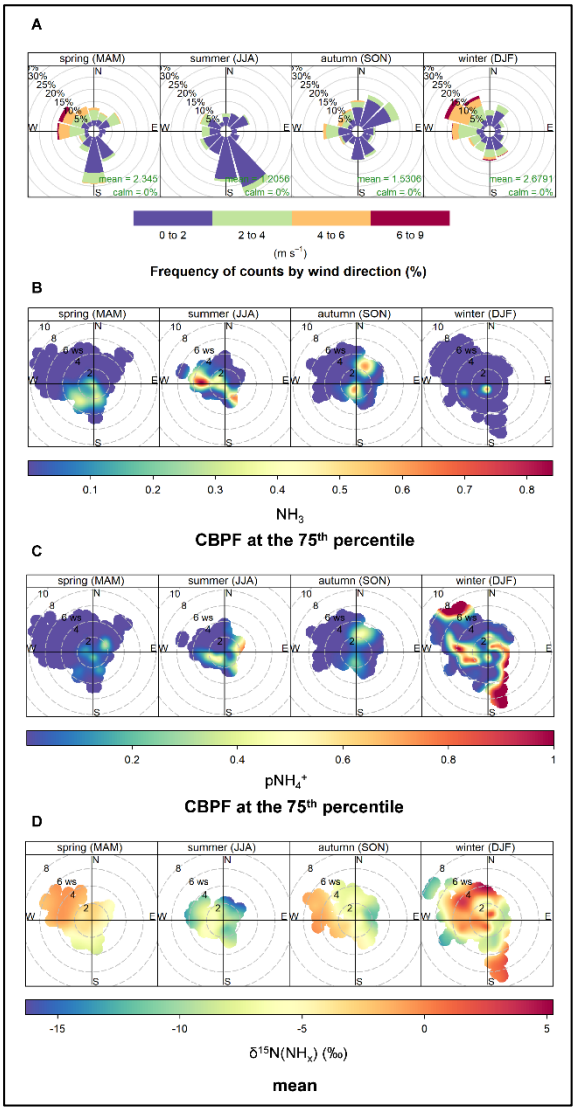

Figure 6. Overview of (A) windrose plots and polar bivariate (wind direction and wind speed) plots of the conditional bivariate probability function (CBPF) for (B) [NH_3] and (C) [pNH_4^+], and (D) mean $\delta^{15}N(NH_x)$ in Providence, RI, sorted by season.

https://doi.org/10.5194/acp-2022-419
Preprint. Discussion started: 24 June 2022

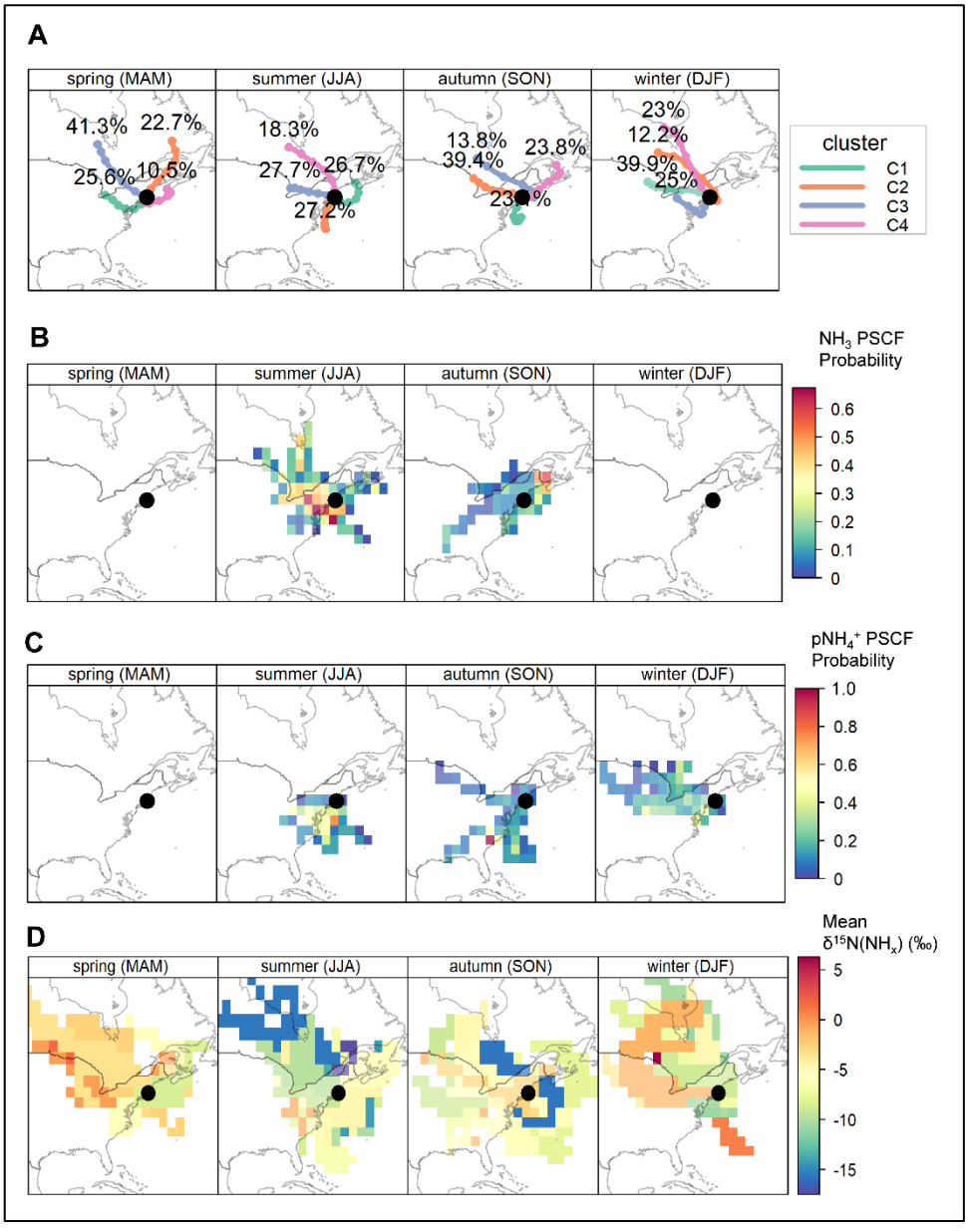

Figure 7. Influence of long-range transport including (A) clustered seasonal air mass back trajectories, (B) seasonal [NH_3] potential source contribution function probability (PSCF), (C) seasonal [NH_3] PSCF probability, and (D) seasonal air mass back trajectory $\delta^{15}N(NH_x)$ mean values.

https://doi.org/10.5194/acp-2022-419
Preprint. Discussion started: 24 June 2022

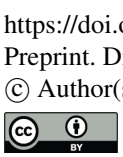

Atmospheric Chemistry and Physics Discussions

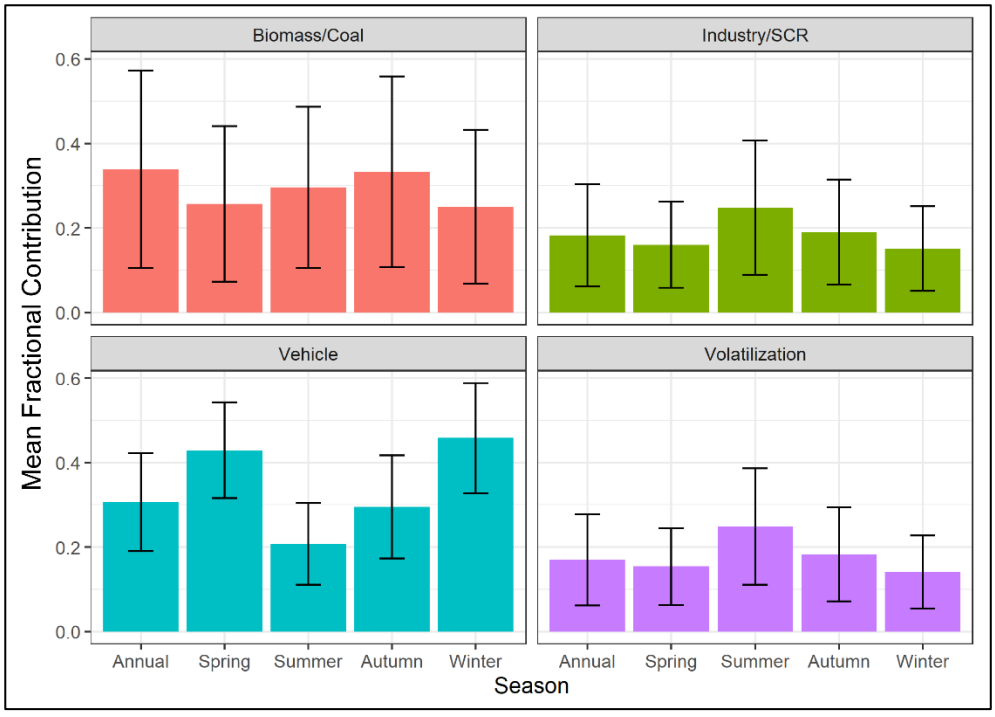

Figure 8. The calculated mean seasonal and annual fractional contribution of emission sources (Biomass/Coal, Industry/SCR, Vehicle, Volatilization) to NH_x in Providence, RI, utilizing a stable isotope mixing model (SIMMR). The error bars represent the standard deviation of the model simulations.

830